Intelligent Knee Sleeves: A Real-time Multimodal Dataset for 3D Lower Body Motion Estimation Using Textile Sensors

Wenwen Zhang[1][*] **Arvin Tashakori**[12]**, Zenan Jiang**[12]**,Amir Servati**[2]**, Harishkumar Narayan**[2]**,**
Saeid Soltanian[2]**, Rou Yi Yeap**[2]**, Meng Han Ma**[2]**, Lauren Toy**[2]**, Peyman Servati**[12][*]

[1]Department of Electrical and Computer Engineering, University of British Columbia
[2]Texavie Technologies Inc.
{wenwenzhang, arvin, jiang, peymans}@ece.ubc.ca
{aservati, harishkumar, ssoltanian, ryeap, meganma, ltoy}@texavie.com

Supplementary Materials

This is the Supplementary Material (SI) for our smart Intelligent Knee Sleeves. The SI is formatted as the following: Appendix A provides more details on the analysis of the wearable knee sleeve data. Equation 1 is the equation we used to quantify the distance between prediction values and ground truth. Figure A1 and Figure A2 is the motion capture outputs and corresponding sensor reaction from our stretchable Knee Sleeves under the scenario that some issues happened to the optical system. Table A1 highlights our contribution to related applications. Table A2 offers a detailed breakdown of how each modality contributes to the overall performance. Figure A4 illustrates the labeling process to obtain the ground truth from a camera-based commercial system. Figure A3 shows the time shift in prediction due to the Bluetooth latency issues. Figure A5 shows the results of unseen tasks in the leg raise pose with seeing 10% of the unseen task's data. Appendix B is the detailed information in the data structure, dimension, and accessibility. Table B5 shows the specific dimension and data we input to the model for training. Table B6 is the number of sessions for each pose and each subject on each day. Table B7 summarizes the list of different exercises we conducted during the data collection process.

Please access the data at https://feel.ece.ubc.ca/smartkneesleeve/. All the data, code, and instructions are stored and can be accessed online in long-term storage repositories. Our work is published under GNU General Public License v3.0.

A Dataset Analysis

Equation 1 is the quaternion distance [1] that we used to quantify the model performance on joints' angel predictions. The $D(q_{pred}, q_{grd})$ is the normalized quaternions presenting the motion of joints of prediction results and ground truth values.

$$
\begin{cases}
D(q_{pred}, q_{grd}) = 1 - <q_{pred}, q_{grd}>^2 \\
<q_{pred}, q_{grd}> = <a_1 a_2 + b_1 b_2 + c_1 c_2 + d_1 d_2> \\
q_{pred} = a_1 x + b_1 y + c_1 z + d_1 w \\
q_{grd} = a_2 x + b_2 y + c_2 z + d_2 w \\
a_1^2 + b_1^2 + c_1^2 + d_1^2 = 1 \\
a_2^2 + b_2^2 + c_2^2 + d_2^2 = 1
\end{cases}
\tag{1}
$$

---

[*]Corresponding authors

(a)

Hip angle (left)

Hip angle (right)

Knee angle (left)

Knee angle (right)

Ankel angle (left)

Ankel angle (right)

Toe angle (left)

Toe angle (right)

Outcome from motion capture system with good performance

(b)

Hip angle (left)

Hip angle (right)

Knee angle (left)

Knee angle (right)

Ankel angle (left)

Ankel angle (right)

Toe angle (left)

Toe angle (right)
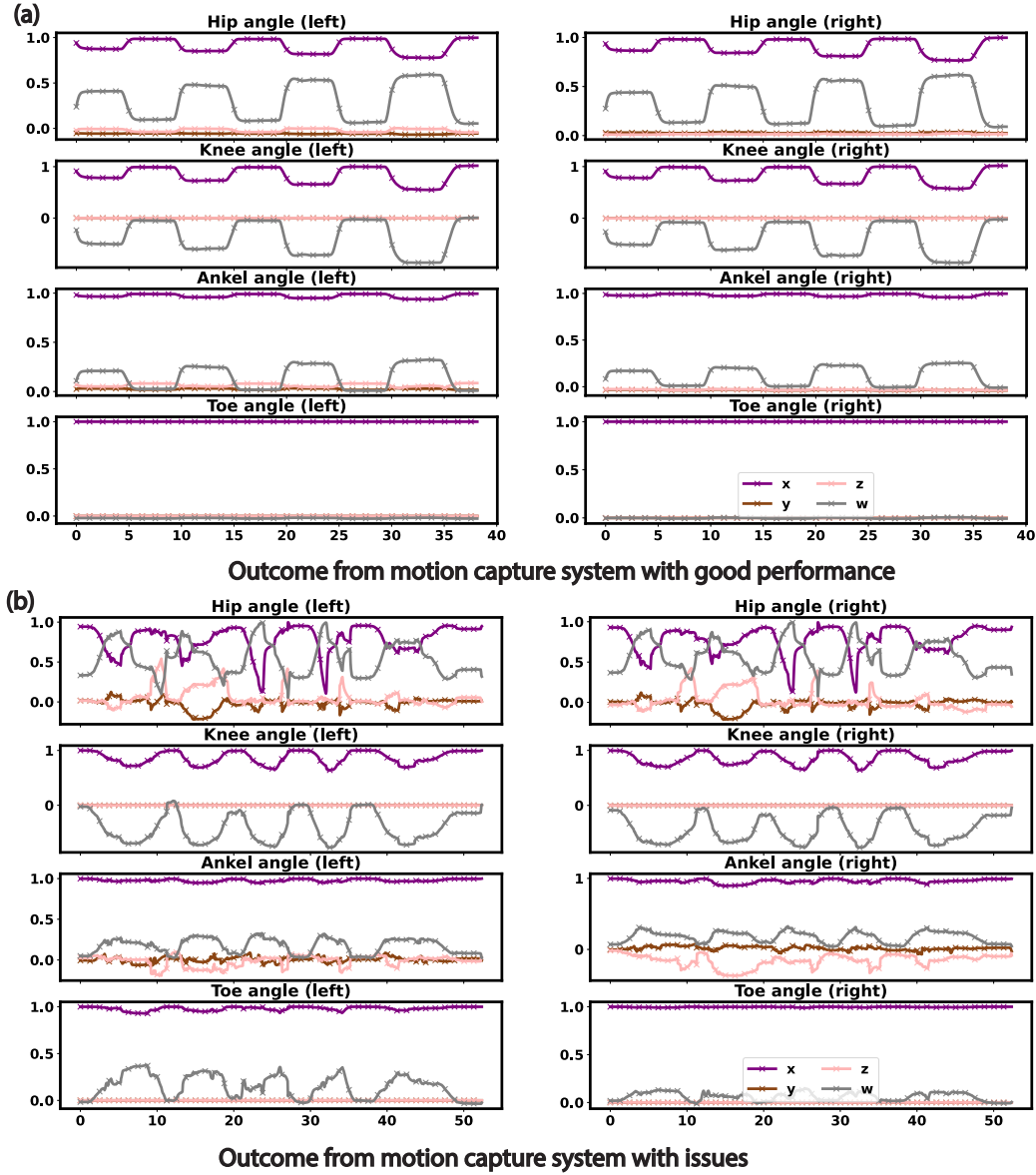
Outcome from motion capture system with issues

Figure A1   Quaternion example from MoCap system of squatting exercise. The environment can significantly impact the performance of the motion capture system, as shown in this illustration. Panel (a) presents ground truth values obtained from a motion capture system that functions smoothly without any hindrances, while panel (b) shows ground truth measurements obtained from the motion capture system that faces various challenges, such as occlusion. The corresponding sensor reaction of the panel (b) is displayed in the Figure A2
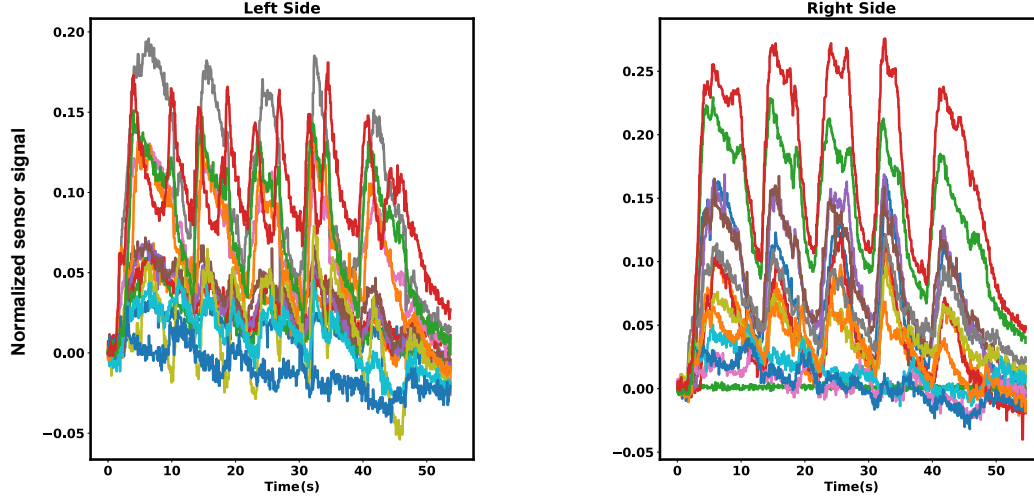
Figure A2 Normalized sensor reaction to the level of pressure applied. Pressure sensor response of the exercise displayed in Figure A1 (b). The strain reaction from the smart Knee Sleeve matches perfectly with the performed exercise without being affected by any environmental issues.

Under adverse environmental conditions, the MoCap system is susceptible to disturbances caused by ambient noise, leading to unstable output. We observed lost and crashed data in the data collection process, as is shown in the Figure A1. Both Figure A1 (a) and (b) are the quaternion outcome from the MoCap system during squatting exercise. Panel (a) demonstrates distinct and coordinated joint motion during the exercise, whereas (b) exhibits a higher level of noise and lacks clear depictions of the quaternion alteration throughout the exercise. The corresponding sensor reaction extracted from our wearable Knee Sleeves after data pre-processing is displayed in Figure A2. The sensor reaction agrees with the squatting exercise, displaying similar patterns as shown in the quaternions illustrated in Figure A1 (a). This validates the failure of the MoCap system to record the joint movements in the exercise during certain environmental conditions. When including labels from MoCap systems like Figure A1 (b) as supervised information in the training, the model training will be affected by less accurate parameters. Conversely, when employing the data represented in Figure A1 (b) as part of the testing set to assess the effectiveness of our baseline model, inaccuracies in the ground truth values will result in higher reported errors compared to the actual values.

Our Smart Knee Sleeve is a stretchable, user-friendly device suitable for long-term outdoor use. We compare our device with a range of wearable devices, highlighting our innovations in Table A1, which includes comparisons with works using only IMUs, textile, and sensor systems fused with IMUs and other flexible sensors. We emphasize our device's simplified setup, cost-effectiveness, and robustness, and its potential for more challenging tasks such as dancing and home fitness.

In our study, we utilize both IMUs and pressure sensors to enhance the accuracy of data measurement and reliability of pose estimation tasks. IMUs, while effective, may experience drift caused by minor errors in acceleration data that accumulate over time. Conversely, pressure sensors are highly sensitive to the kinesthetic feedback of joints, even with micro-movements. They can directly detect local deformations, including stretches and pressures of the skin and muscle tissues, caused by joint movements. The fusion of data from IMUs and pressure sensors in our algorithm provides a more comprehensive understanding of the poses. A crucial factor to consider is that IMUs located around the knee joints alone are insufficient to support the predictions of other joints. The pressure sensor we employ can detect muscle activities around the thigh and shank, thereby supporting the prediction of nearby joint activity, such as the hip and ankle. Furthermore, both IMUs and pressure sensors are reliable sources of kinesthetic information under a wide range of conditions, including outdoor, low-light, noisy, and cluttered environments. For a direct comparison demonstrating how the combination of IMU and pressure sensor data results in superior prediction accuracy, We carried out an experiment demonstrating that by integrating multimodal data from both IMUs and pressure sensors, we achieve enhanced accuracy in Table A2.

3

Table A1 Comparison table of related work.

	Sensors Type	Integrated Device	Wireless Steaming	Task	Multi-person scenario issue	Avg RMSE
Our work	IMUs, textile	y	y	Joint orientation inference	n	7.21 deg (Avg angle error)
Luo et al. (2021) [2]	Textile	y	n	Pose classification	n	na
DelPreto et al. (2022) [3]	IMU,EMG tactile, camera	n	n	Activity classification in ketch	n	na
Luo et al. (2021) [4]	Tactile	y	n	21 keypoint estimation, activity classification	y	6.9 cm (Avg location error)
Tan et al. (2022) [5]	IMUs	n	nm	knee flexion/extension prediction	n	9.52 deg (Avg angle error)
Huang et al. (2018) [6]	IMUs	n	nm	Pose estimation	n	15.84 deg (Avg angle error)

[*] na: not applicable; nm: not mentioned.

Table A2 RMSE in degree unit for smart Knee Sleeve performance. This supplementary materials provide detailed information on how the multimodal data contributes to the model performance. When training with synthesized data from both IMUs and pressure sensors, we achieved the highest accuracy in the prediction task.

Training Data	LHip	LKnee	LAnkel	LToe	RHip	RKnee	RAnkel	RToe
IMUs Pressure sensor	9.03	11.8	6.23	3.81	9.31	7.69	7.04	2.77
Pressure sensor	14.06	15.76	15.60	4.80	13.32	14.54	8.01	5.49
IMUs	11.76	11.17	14.80	4.79	10.85	11.29	6.63	5.54

The latency and shift in predictions caused by Bluetooth and communication systems are illustrated in the Figure A3. The utilization of Bluetooth technology can introduce irregular intervals in wearable recordings, consequently impacting the precision of predictions due to discrepancies between the data extracted from our flexible electronics and the ground truth values from MoCap. The comparison of predictions and ground truth data in Figure A3 shows that while the estimated amplitude and frequency of quaternion alteration match well with the ground truth data, there is a noticeable phase shift over time that becomes more severe as time passes by.

Figure A4 illustrates the label generation process as we mentioned in the section 3. We collect the time-series data recording joints movement from the MoCap system as the supervision information for the later training process.

We illustrate a noticeable decline in model performance when dealing with unseen tasks, as shown in in Figure 6(g-i), and additionally, we perform experiments where the model is exposed to only a restricted portion of labels in Figure A5. We split 90% of the leg raise data as testing and let the model see 10% of leg raise data during the training process. The Figure A5 (a) is the result of our baseline model that hasn't seen any leg raise data, while Figure A5 (b) shows the outcome from the model that is trained with 10% of leg raise data. We can observe an obvious improvement in the major joints such as the knee and thigh ankle for the left and right sides separately after only seeing a small portion of the data that comes from the leg raise pose.

We summarized the RMSE in degrees for more details in the seen and unseen task as a supplementary for the Table 1. In all seen scenarios, Bend squat may only take a small portion in the test set due to

Table A3 RMSE in degree unit for smart Knee Sleeve performance. This supplementary materials provide detailed information in the Table 1, including the separate RMSE errors for squat, hamstring, and leg raise poses for all seen scenarios.

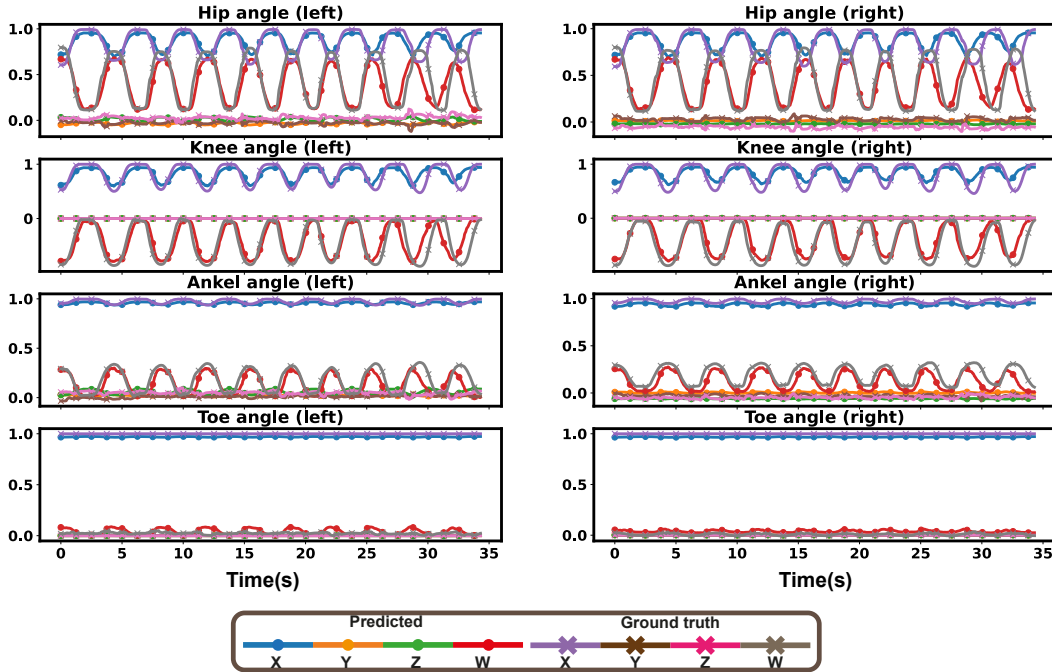| Scene	Poses	LHip	LKnee	LAnkel	LToe	RHip	RKnee	RAnkel	RToe	Avg
All_seen	Squat	9.90	10.20	5.18	3.96	9.59	7.91	7.39	3.14	7.16
	Hamstring Curl	5.59	18.21	7.01	3.40	9.59	4.41	4.86	1.19	6.78
	Leg Raise	8.26	8.09	8.97	3.57	7.45	9.55	7.65	2.30	6.98
	Avg	9.03	11.8	6.23	3.81	9.31	7.69	7.04	2.77	7.21
Unseen Tasks	BendSquat	17.5	14.20	12.30	4.25	17.90	15.10	12.10	5.12	12.31
	Hamstring Curl	12.7	18.00	6.13	2.71	12.40	16.90	6.49	4.13	9.93
	Leg Raise	10.20	19.80	9.05	2.56	9.55	16.20	9.29	5.50	10.27
	Avg	12.91	18.13	9.20	3.06	12.70	16.16	9.32	5.05	10.82

Figure A3 Quaternion comparison from ground truth and predictions in time unit (second). Due to the Bluetooth issue, the predictions are subject to shifting caused by wireless communication latency, and this shift becomes progressively more severe over time.

random sampling, we use overall squatting pose for error calculation here. The joint predictions for different poses display close values in all seen scenarios.

We provide videos with 3D human models from MoCap ground truth values and our smart Knee Sleeve recordings for comparison in the attachment. The pink dummy in the video is reconstructed from the MoCap values and serves as the ground truth in the video. The blue figure is restored from our smart Knee Sleeve predictions. We provide examples for squatting, hamstring curl, and leg raise poses separately. In the squatting poses, we present RGB camera views, MoCap software recordings, and 3D human model predictions for reference. While the ground truth and our model prediction comparisons are provided for leg raise and hamstring curl poses. The evident correspondence between the ground truth and prediction reconstructions of 3D human model visualizations provides validation for the efficacy of our hardware and model in accurately tracking human activities.
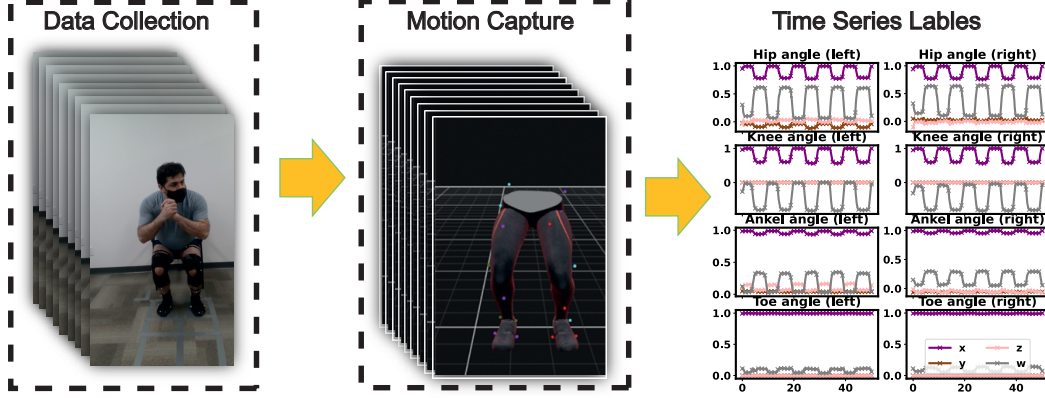
Figure A4   Overview of the label generation process (Squat pose). We obtain the ground truth label by utilizing a camera-based MoCap system that incorporates markers attached to the primary joints of the lower body. The outcome of this system is 16-dimensional quaternion data that accurately represents the motion of the major joints.
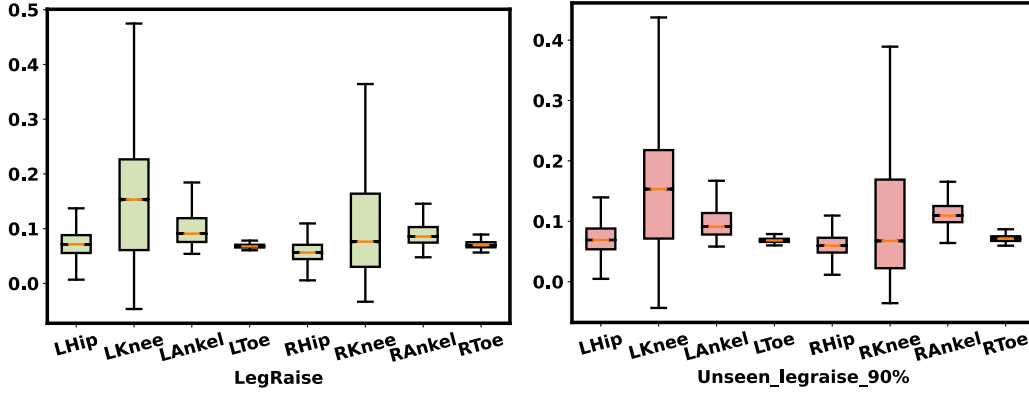

Figure A5   Quaternion distance comparison from unseen tasks. When we feed in a limited number of leg raise data (10%) with setting position as a start point, the outcomes increased compared to the performance that hasn't seen any leg raise data.

We provide the Mean Squared Derivative (MSD) and derivative of prediction quaternions in Table A4 and Figure A7 to measure the smoothness of our model performance. Our prediction data are quaternions scaled from 0-1, and the MSD for each orientation is at the scale of 10^{-4}, which proves our prediction results don't have abrupt changes and are smoothly transitioned.

B   Dataset Summary and Accessibility

Structure of the dataset: Our dataset provides information on synchronized wearable data recordings for smart stretchable Knee Sleeves and camera-based annotations from the MoCap system. The main exercises we focus on are squatting, hamstring curl, and leg raise pose. The structure of the folder is arranged as follows. The data structure is displayed in the Table B5. We have a total of 32-dimensional data collected from the smart Knee Sleeves. The output is 21-dimensional data representing the quaternions of major joints on the lower body.

Table A4   Mean Squared Derivative results for quaternion predictions on all orientations

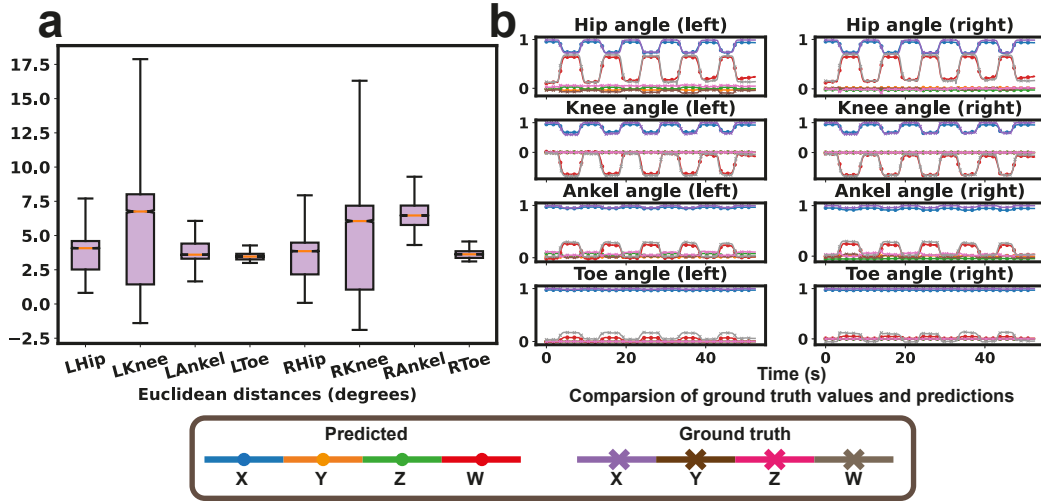| Orientation	x	y	z	w
MSD	6.92e-05	9.82e-09	7.08e-09	5.46e-04

Figure A6 Estimation results comparison. (a). The model's overall performance in Euler angles. (b). The quaternion output from the models. The knee angle prediction showed the highest level of accuracy across all joints. The toe angle was found to be mostly stable with minimal movement during the squat exercise.

- dataset/
  - D0/-D11/
  - This folder contains the data files collected from various days. Since each day includes independent calibration of the MoCap system, this may bring in extra noise.
    * P0/-P5/
    * In this directory, we include files collected on the same day from various subjects. It's worth noting that different participants wore knee sleeves of varying sizes on that particular day.
    * This folder contains three types of files:
      · Exercise.csv. Example: BendSquat.csv
      · Exercise_l.csv. Example: BendSquat_l.csv
      · Exercise_r.csv. Example: BendSquat_r.csv
      · Exercise.csv files are ground truth annotations collected from the motion capture system, while Exercise_l.csv and Exercise_r.csv are readouts from the smart Knee Sleeves of the left and right sides of the body separately. The data structure is displayed in Table B5

The summary of Table B6 contains the content of the number of tasks performed by each subject and the number of subjects collected each day. Squatting exercises usually are comprised of several different types of tasks, but we term them as squat together in this table. Please refer to the Table B7 for details of a full list of various exercises we have conducted. In Table B7, Exercise column is the name of the exercise we guide the participant to do during the data collection process. #Total-files column is the total number of files we have with each corresponding exercise, which contains Mocap ground truth data, and the smart Knee Sleeve data for the left and right sides separately. We have one missing side file for the hamstring pose due to battery issues. #Session column summarizes the sessions we have for each exercise.

Table B5 Data Structure for the wearable benchmarks used in this paper. The last quaternion columns are the relative values calculated from $Quat_0$ and $Quat_1$ attached to the thigh and shank separately.

Data	Time	Pressure Sensor Pins	Acc0	Quat0	Gyro0	Acc1	Quat1	Gyro1	Quat
Dimension	1	14	3	4	3	3	4	4	4

Table B6 Details about our smart Knee Sleeve dataset including data collection dates, number of subjects, and tasks. Squatting tasks usually contain multiple categories of tasks, but we refer to them as squatting in general. Please refer to Table B7 for a full list of exercises.

Date	Subject	Tasks			Summary
		Squat	Hamstring Curl	Leg Raise	
D0	P0	6	1	1	8
D1	P0	5	1	2	8
D2	P0	7	2	2	11
D3	P0	5	1	2	8
	P3	6	0	2	8
D4	P0	7	2	2	11
D5	P0	4	2	2	8
D6	P0	1	1	0	2
	P1	2	0	2	4
D7	P0	8	2	2	12
	P2	6	1	2	9
D8	P0	8	2	2	12
	P1	5	2	2	9
	P4	3	2	1	6
D9	P0	5	1	2	8
	P1	8	2	2	12
D10	P0	7	2	1	10
	P1	5	2	2	9
D11	P0	6	0	0	6
	P1	2	0	0	2
	P5	1	0	0	1

Table B7 Detailed list of exercises collected with our smart Knee Sleeve dataset.

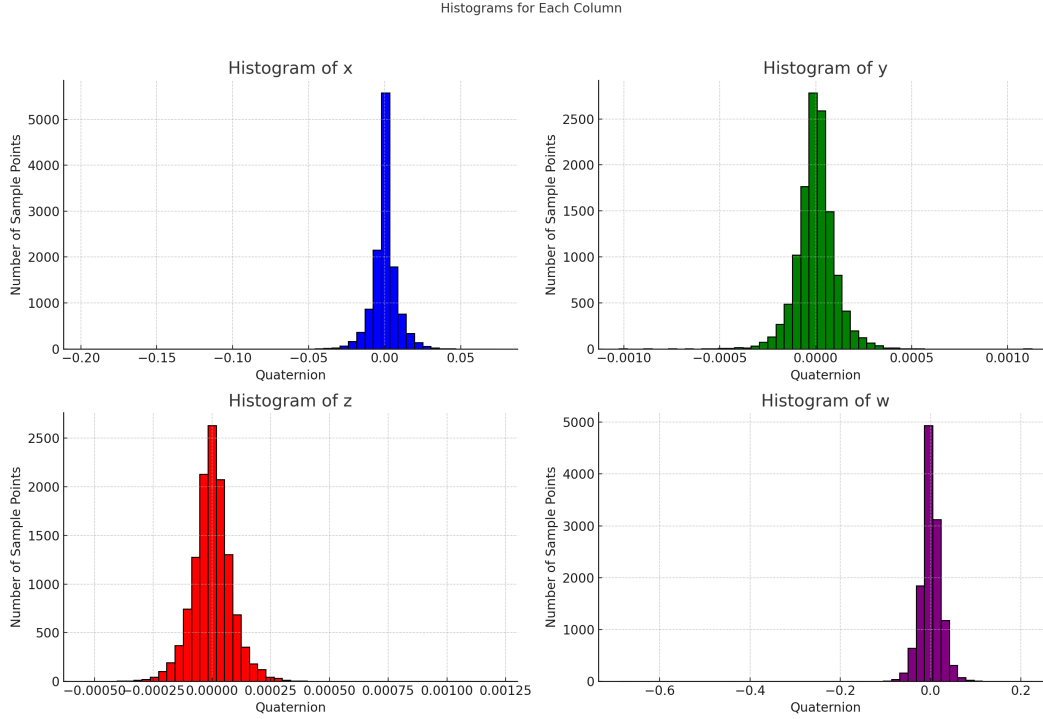| Exercise	# Total files	# Sessions
AppFastSquat	3	1
AppSlowSquat	3	1
FollowSquat	3	1
HamstringCurlLeft	44	15
LegRaiseLeft	48	16
StepwiseSquat	45	15
TiredSquat	27	9
ToeOutSquat	3	1
BendSquat	48	16
LegRaiseRight	45	15
SlowSquat	45	15
Squat	75	25
WeightSquat	48	16
HamstringCurlRight	33	11
StaggeredRightSquat	9	3
PulseSquat	6	2
StaggeredLeftSquat	6	2
Rest-l	2	1
Rest-r	2	1

Figure A7   Derivative for quaternion predictions on all orientations.

C   Ethical Considerations

Participants were fully informed of the study's purpose, potential risks, and benefits. Personal information was kept confidential, and data were used exclusively for research purposes. Our wearable sensors were designed to be safe, minimizing discomfort and skin irritation. We monitored participants to prevent extended use of sensors that could cause skin irritation. We also complied with data protection laws by securely storing all collected data and taking measures to prevent unauthorized access. Our study was conducted ethically and responsibly. The product of our Intelligent Knee sleeves and its related data are the intellectual property of Texavie Technologies Inc. Please refer to Texavie for more details.

References

[1] Du Q Huynh. Metrics for 3d rotations: Comparison and analysis. *Journal of Mathematical Imaging and Vision*, 35:155–164, 2009.

[2] Yiyue Luo, Yunzhu Li, Pratyusha Sharma, Wan Shou, Kui Wu, Michael Foshey, Beichen Li, Tomás Palacios, Antonio Torralba, and Wojciech Matusik. Learning human–environment interactions using conformal tactile textiles. *Nature Electronics*, 4(3):193–201, 2021.

[3] Joseph DelPreto, Chao Liu, Yiyue Luo, Michael Foshey, Yunzhu Li, Antonio Torralba, Wojciech Matusik, and Daniela Rus. Actionsense: A multimodal dataset and recording framework for human activities using wearable sensors in a kitchen environment. *Advances in Neural Information Processing Systems*, 35:13800–13813, 2022.

[4] Yiyue Luo, Yunzhu Li, Michael Foshey, Wan Shou, Pratyusha Sharma, Tomás Palacios, Antonio Torralba, and Wojciech Matusik. Intelligent carpet: Inferring 3d human pose from tactile signals. In *Proceedings of the IEEE/CVF Conference on Computer Vision and Pattern Recognition*, pages 11255–11265, 2021.

[5] Jay-Shian Tan, Sawitchaya Tippaya, Tara Binnie, Paul Davey, Kathryn Napier, JP Caneiro, Peter Kent, Anne Smith, Peter O'Sullivan, and Amity Campbell. Predicting knee joint kinematics from

wearable sensor data in people with knee osteoarthritis and clinical considerations for future machine learning models. *Sensors*, 22(2):446, 2022.

[6] Yinghao Huang, Manuel Kaufmann, Emre Aksan, Michael J Black, Otmar Hilliges, and Gerard Pons-Moll. Deep inertial poser: Learning to reconstruct human pose from sparse inertial measurements in real time. *ACM Transactions on Graphics (TOG)*, 37(6):1–15, 2018.